A performance evaluation of three high-fidelity streak cameras

James D. Bonlie and Mark E. Lowry

Lawrence Livermore National Laboratory
P.O. Box 808, Livermore, California 94551

ABSTRACT

Several scientific programs at Lawrence Livermore National Laboratory (LLNL) require instrumentation that can capture optical signals with high fidelity. Typically, they require high temporal resolution, high spatial resolution, and high dynamic range. The instrument of choice for most of these multichannel, data-recording applications is the optical streak camera. We have evaluated three optical streak camera systems under similar conditions: (1) the EG&G model L-CA-15 streak camera, designed and built under U.S. Department of Energy (DOE) contract, with a streak tube designed for a time response of a few picoseconds; (2) an in-house (LLNL) design, with an ITT F4157 streak tube that operates in the extraction mode; and (3) a Thomson-CSF model TSN 506 streak camera, with an ITT F4157 streak tube that also operates in the extraction mode. All three systems were found to be capable of time response better than 40 ps FWHM, a dynamic range of greater than 100, and spatial resolution greater than 5 line pairs per millimeter (lp/mm). The experimental setup and plots of results are presented and discussed.

1. INTRODUCTION

As a result of recent streak-tube computer modeling and studies at LLNL, it was established that the ITT F4157 streak tube could be used for 5-GHz operation when the temporal page length was near 7.5 ns across a 40-mm phosphor screen.[1] Based on these modeling studies, a camera was designed and constructed for various applications at LLNL. Complementary 800-V deflection circuits with 5-ns transitions and a −2250-V gating circuit were designed for the camera. An LLNL Nuclear Test Program downhole camera chassis was used to house the new electronics and streak tube [see Fig. 1(a)].

EG&G has built several complete cameras, including streak tubes, at its Amador Valley Operations facilities in Pleasanton, CA. The basic camera design is over 2 years old and has been evaluated for various LLNL applications [see Fig. 1(b)]. These cameras were designed for use in LLNL experiments and in support of other DOE programs. From results of tests performed by EG&G at Los Alamos, NM, one of the earlier EG&G cameras was claimed to have demonstrated time resolutions as low as 62 ps with 50-ns/40-mm deflection.[2] For the evaluation reported in this paper, the camera's deflection circuitry was modified to provide a sweep rate similar to the other two cameras being evaluated.

The first Thomson-CSF streak camera to contain an ITT F4157 streak tube was made available for this comparison. A model Thomson-CSF TSN 506 P picosecond plug-in was used to achieve a 5-ns sweep rate. This camera has undergone similar testing here at LLNL and has demonstrated time resolution as good as 20 ps during a 5-ns/40-mm deflection period.[3] This camera is the result of a joint effort by LLNL, Thomson-CSF (Paris, France), and TEAM Systems (Santa Clara, CA) [see Fig. 1(c)].

Figure 2 defines the one basic system used to evaluate all three cameras for temporal resolution, spatial resolution, and dynamic range. Because we required a fast optical impulse to perform our comparisons, we used a mode-locked dye laser with a continuous pulse train for the optical source. To characterize the light pulses, which were 10 ps FWHM at a 593-nm wavelength, we used a scanning autocorrelator. An etalon provided known timing and variable optical pulse intensities. A series of lenses, ending with a cylindrical lens, line-focused the laser light to the photocathode of the streak camera under test. A photographically etched mask placed on the photocathode of each camera simulated data channels that would be optical fibers in normal applications. At the output of the streak tubes were ITT F4113, 40-mm-diameter microchannel plate intensifier tubes (MCPIs). A high-resolution,

Figure 1. (a) LLNL/ITT prototype streak camera. (b) EG&G L-CA-15 streak camera. (c) Thomson-CSF 506 streak camera. (All cameras have MCPIs.)

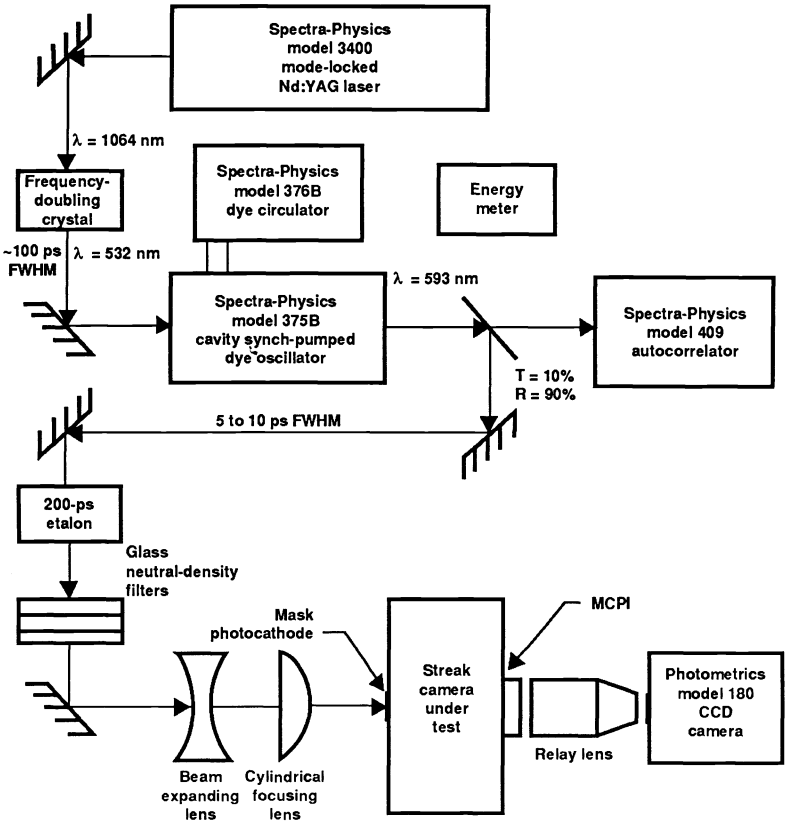

Figure 2. Multichannel streak camera characterization system.

high-dynamic-range (14-bit A/D) Photometrics Ltd. CCD camera readout system was used for image capture. The record lengths from this system were in the 4- to 5-ns range. Each record contained information on temporal impulse response, spatial resolution, and dynamic range. Immediate digitization of the many acquired streak-camera images made analyzing the data considerably easier compared to film recording.

2. A BASIC COMPARISON OF THE EG&G AND ITT STREAK TUBES

The two types of streak tubes used in this evaluation are considered "large format," in that they can accept a large signal population along the spatial direction of the input photocathode. The ITT tube (see Fig. 3) is 24.8 cm in overall length and has an S-20 photocathode and a P-20 phosphor screen with an internally curved fiber input optic and a flat fiber output optic. The first accelerating potential is introduced by the curved (extraction, gating, or acceleration) electrode, about 6 mm from the photocathode surface. This electrode consists of a disk with a 7×30-mm rectangular aperture that defines the usable area of the photocathode. Since this tube has a flat phosphor screen, the input image is not uniformly focused across the output phosphor plane because of the varying distances that the photoelectrons must travel.

The EG&G tube (see Fig. 3) is 31.1 cm in overall length and has an S-20 photocathode deposited on the internally curved surface of the input fiber-optic window. The output fiber-optic window has an internal, 1.5-in. radius of curvature that was designed to provide a uniformly focused image across the P-20 phosphor screen. Both this tube and the ITT F4157 tube invert the image. The EG&G tube employs a disk-shaped first electrode similar to that of the ITT tube (although it is much closer to the photocathode), and the dimensions of the aperture are 1×48 mm. The long dimension of the slotted apertures in the disks of both tubes defines the usable length for input data channels (i.e., spatial information).

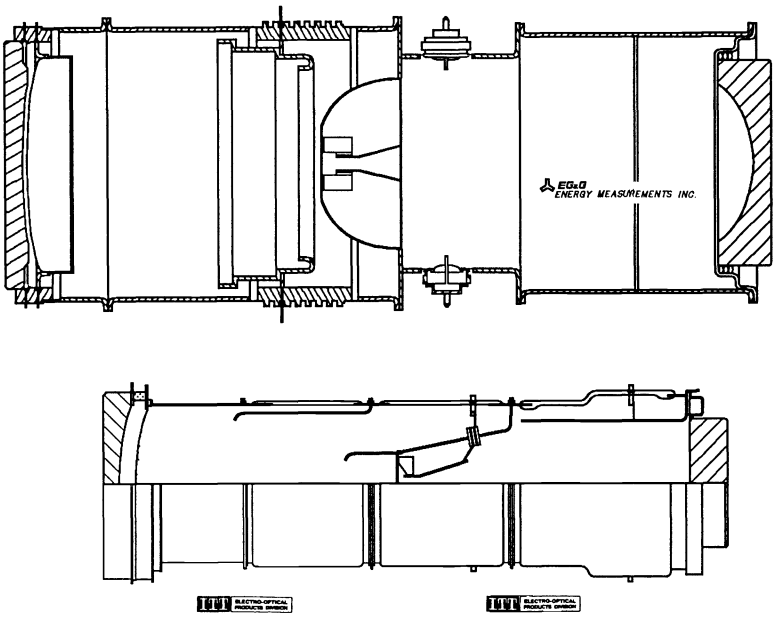

Figure 3. EG&G Energy Measurements streak tube (top). ITT Electro-Optical Products Division streak tube (bottom). Scale is not exact.

The geometry and position of the electrode closest to the photocathode constitute a major difference between the ITT and EG&G tubes. The EG&G tube was designed to rapidly accelerate the photoelectrons that come off the photocathode by applying about 700 V across the short distance (~1 mm) between the photocathode and the accelerating electrode. Some of the aberration introduced by the narrow slot of the accelerator grid is removed by back-biasing the deflection plates in the tube.[2] The effect of the remaining aberration is that some of the spatial resolution is sacrificed for a reduced image width along the temporal axis of the output screen. This is what EG&G calls $M = 0$ (magnification equals zero) in the time direction.

In both the LLNL and Thomson-CSF cameras, the ITT tubes are operated far from their original electron-optics design. The ITT tube was originally designed to be used as a streaked image tube with a relatively low field gradient between the photocathode and the first electrode (see Fig. 3).[4] For an ITT tube operated in the extraction mode, a cylindrical electron lens with a high field gradient forms near the first electrode. The photocathode-to-accelerator electrode potential in this tube needs to be about 2250 V because the spacing between these electrodes is larger than in the EG&G tube. "Extraction mode" refers to the application of a large voltage potential near the photocathode surface to rapidly accelerate the photoelectrons, which reduces the transient time spread of the electron emissions.

Another important difference between the operating parameters of these cameras is the overall streak-tube acceleration potential. For both tubes, the photocathodes are at the highest negative potentials, with the phosphor (anode) at ground potential. The EG&G tube can operate with an overall potential from 15 to 30 kV as designed, although for this test, the maximum voltage was 20 kV. Radiant gains of all these imaging streak tubes are found to be around 30 at peak photocathode quantum efficiency (QE) when the overall streak-tube acceleration potential is 15 kV (Ref. 5). The ITT tubes were designed and operated at a maximum potential of 15 kV. The radiant gain of the EG&G tube could be over 40% higher than either ITT tube because of its higher accelerating potential. These estimations are based on P-20 phosphor emissions of 0.05 photons per electron per volt of electron acceleration and a photocathode QE of 10% at 520 nm. Absolute radiant gain measurements were not made for this evaluation.

We found the image magnification of the cameras (output to input) along the spatial axis to be 1.24 for the Thomson-CSF 506 camera, 1.34 for the LLNL/ITT model, and 0.975 for the EG&G camera.

MCPIs must be used at the output of all these streak tubes to adequately expose the readout device while keeping the input radiant flux density at the streak-tube photocathode low enough to prevent excessive space-charge effects.[6,7]

3. ASPECTS OF THE COMPLETE STREAK CAMERAS

All of the cameras are "gatable," a requirement for many applications at LLNL, because the user must be able to select the desired period of data acquisition while preventing an overwritten image during deflection retrace. The cameras are capable of various gate-pulse widths. The gating (unblanking) pulse in the EG&G camera has a rise time of about 40 ns (0 to 100%), a duration that is prescribed by the sweep rate (5 to 10 ns minimum), and a fall time of about 350 ns. This gating is accomplished with a pulse amplitude of about −700 V peak that is capacitively coupled to the streak tube's photocathode. A fixed resistive divider string inside the EG&G streak tube's potted housing statically biases the tube OFF; therefore, the EG&G camera requires a gate pulse to allow the photoelectrons to leave the photocathode. The camera can be focused by triggering the gate at a high rep rate (up to 500 Hz), which would appear similar to a static ON mode, although the image will become somewhat unfocused during the transition periods.

The LLNL/ITT and Thomson-CSF cameras have focus modes that change the resistive divider string and can be used to bias the streak tubes ON while statically focusing the cameras. The LLNL/ITT camera has a −2250-V gating pulse with a 200-ns rise time (0 to 100%), a pulse duration that lasts a minimum of about 20 ns, and a fall time of about 400 ns. The gating circuit consists of a planer triode in a common cathode configuration. The Thomson-CSF/ITT camera also uses a planer triode for the gating device, which provides a −2250-V pulse that has an 80-ns rise (0 to 100%), a minimum duration of 300 ns, and a 400-ns fall time. The gate circuits in both the LLNL/ITT and Thomson-CSF cameras typically would be operated only in a single-shot mode, although a slow rep rate is allowed.

The external power supplies of the EG&G camera are similar to those used for the LLNL/ITT prototype camera. These cameras require a number of low-voltage inputs—including 5, 15, and 28 Vdc—for a combined total power consumption of about 34 W. The Thomson-CSF camera is fully self-contained, with 110 Vac (60 W) being the only input supply.

The EG&G camera typically has selectable sweep rates that allow the deflection across a 40-mm page to be 25, 50, 100, 200, 400, and 500 ns. Intermediate and slower rates can be provided by some internal adjustments. The Thomson-CSF camera, using a model TSN 506 P picosecond unit, has a plug-in module that is used to select 2, 5, 10, or 20-ns deflection periods across the 40-mm output. The LLNL/ITT camera has a fixed, 5-ns sweep rate, although the circuitry can be modified to accommodate other rates.

4. EXPERIMENTAL SETUP

The following discussion describes the typical test setup we used to evaluate all three streak cameras. The streak cameras with their associated MCPIs were the only components that changed.

The heart of the Spectra-Physics laser system consists of a Nd:YAG medium that is pumped with a CW krypton arc lamp. An acousto-optic modulator permits mode locking of the laser-light pulses at an 82-MHz rate (12-ns pulse separation). The 1.06-m, TEM-00, mode-locked pulse train consists of 80- to 100-ps FWHM pulses with an average power of about 7.5 W. A doubling crystal is used to convert the 1.06-μm light into 532-nm light. The resulting pulses are then used to synchronously pump a mode-locked cavity dye laser. The mirror cavity associated with this unit must have the same length as the Nd:YAG cavity to be synchronously pumped. The output pulses from the dye laser cavity are from 5 to 10 ps FWHM (depending on cavity length, drift, and alignment), with an average power ranging from 200 to 400 mW and a 593-nm wavelength. An electronic pulse from the laser mode-locker unit was used to synchronize the triggering of the streak and CCD cameras.

The optical pulse train is then divided by a 10/90 beam splitter, with the smaller portion being monitored with a Spectra-Physics scanning autocorreletor. Most of the light was sent to an etalon to generate a decaying

pulse train from each mode-locked optical pulse. The etalon has 70% reflective internal surfaces, which are spaced to produce a train of pulses separated by 200 ps, with intensities that exponentially decay by approximately a factor of 2 with each pass. Placed after the etalon were neutral density (ND) filters, which were used to moderate the energy level of the pulse train. The light was then sent through a beam-expanding lens to increase the usable diameter. A cylindrical lens was used to collapse the y-axis of the beam and increase the power density along the spatial input axis to the photocathode of the streak camera under test. This resulting footprint was line focused on the mask located on the streak-camera photocathode.

The mask taped over each photocathode input window consisted of a row of squares 100 μm on a side, positioned with 200-m center-to-center spacing (i.e., a spatial frequency of 5 lp/mm) along the spatial direction, parallel to the length of the accelerating electrode slot of each tube. The emulsion side of the film mask was placed against each window. This proximity-focusing method can reduce the possibilities of light leakage and fore-optic lens misalignment.

Mask alignment for both types of tubes was important so that the photoelectron emissions were centered along the accelerator grid slots. For placement of the mask, we used a caliper to map the slot with reference to the streak-camera chassis. It was possible to look through the semitransparent photocathode windows and see a diffuse image of each slot.

An efficient, high-resolution, Tinsley 2.5:1 reducing relay lens was used to interface the CCD to the streak camera system.[8] Some properties of the lens include a 5.1% total energy transfer, 0.245 input numerical aperture with an image resolution of $>$0.7-MTF for 22 lp/mm at the objective.

The CCD chip is a Thomson-CSF 576 x 384-pixel array format. Each individual pixel is 23 μm on a side. As a result of the lens-reduction ratio, the individual CCD pixels mapped to squares 57.5 μm (23 μm x 2.5) on a side on the MCPI output screen. Since the CCD has 576 data points on the time axis of the readout, only about 33 mm of the image on the MCPI phosphor was recorded. On the spatial axis, 384 CCD pixels map to about 22 mm across the MCPI phosphor. The MCPI phosphor screen area was not fully used, although the diagonal of the image was about 40 mm. Note that if film had been used as the readout medium, then the entire 40-mm window area could have been used.

It is important to define the sweep rate (typically ns/mm) or the record length for each camera. This information is necessary when considering the resolution effects of the MCPI and the CCD. The sweep rates were determined through data analysis by using the known 200-ps timing of the etalon pulse train. The approximate time per pixel was then determined for the given CCD readout. The record lengths for each camera are as follows:

- EG&G camera—33 mm $\propto$ 4.7 ns record length (averaging 8.2 ps/CCD pixel)
- LLNL/ITT camera—33 mm $\propto$ 4.4 ns record length (averaging 7.6 ps/CCD pixel)
- Thomson-CSF 506—33 mm $\propto$ 4.1 ns record length (averaging 7.1 ps/CCD pixel)

5. PROCEDURES

The CCD camera was oriented so that the columns of the array were nominally aligned along the time direction of the streak-camera output image (i.e., the rows of the array were aligned along the spatial direction of the image). Once the system was set up and operational, the image from the streak camera was focused onto the CCD. These adjustments were critical because the relay lens has an extremely short depth of field.

For each camera, background images were acquired just prior to data acquisition. For each background image acquisition, the cameras and MCPIs were fully powered and gated with the light source removed.

A series of image acquisitions were performed for each streak camera. The data acquisition and archival proceeded rather quickly when all components were operational. The main system variables were laser-power and pulse-width fluctuations, light-level adjustments made with ND filters, and the gain setting of the MCPIs. The pulse width and average power of the laser were monitored before each captured image.

The CCD camera was controlled by an LSI-11/73 computer during data acquisition. The stored images were transferred via an Ethernet local area network to a MicroVAX computer for processing. The processing was handled using Imaging Data Language (IDL), a product of Research Systems, Inc. The background of each image was subtracted, after which the portion of the image that had no discernable data was removed. The resulting images were then 301×383 pixels in size.

Data analysis becomes simplified if the swept image on the streak-camera phosphor is parallel to the CCD-array column direction. Because of the mechanical constraints of the setup, it was not convenient to rotate either the CCD camera or the streak cameras prior to data acquisition. This prevented precise alignment of the streak-camera images to the axes of the CCD array. During data analysis, IDL was used to rotate these images 1 or 2 deg, as necessary, in order to square the images in memory.

6. EXPERIMENTAL RESULTS

In Fig. 4 are representative streak camera images obtained with our multichannel temporal characterization system. The image in Fig. 4(a) was obtained with the EG&G camera, and that in Fig. 4(b) with the Thomson/ITT camera; increasing time is down, while the spatial direction is horizontal. The decaying etalon pulse train is very well resolved in the temporal direction (with 200 ps separation), and the individual input channels from the input mask are in evidence but not as well resolved. Spatial magnification differences are apparent when the two images are compared. The pulse train appears with higher intensity near the spatial center of each frame. This is mainly a result of a combination of the nonuniform laser-pulse footprint and spatial roll-off of the relay lens.

We examined the spatial resolution of the three cameras by extracting temporally narrow portions (three rows) of the streak camera records. These portions were centered at the temporal peaks of the etalon pulse train and covered the entire spatial extent of the streak camera record, which was limited by the size of the CCD array. We analyzed the spatial information by averaging the CCD rows. Typical data is shown in Fig. 5, where we present data from all three cameras at approximately the same intensity. The peaks correspond to the open areas of the photocathode masks, while the valleys represent the dark areas. From this data, one may infer the streak-tube magnifications and the spatial contrast at the mask frequency of 5 lp/mm. At this frequency, the Thomson/ITT camera appears to have better resolution than the LLNL/ITT and EG&G cameras.

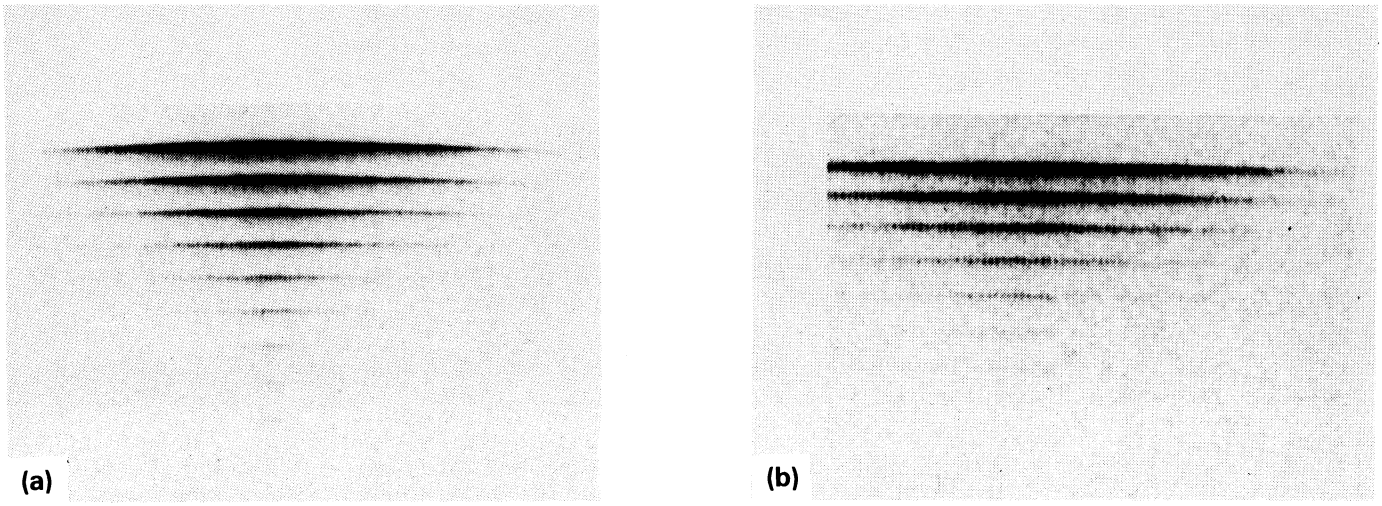

Figure 4. (a) An example image from the EG&G camera obtained by using our multi-channel temporal characterization system. (b) A similar image from the Thomson-CSF camera.

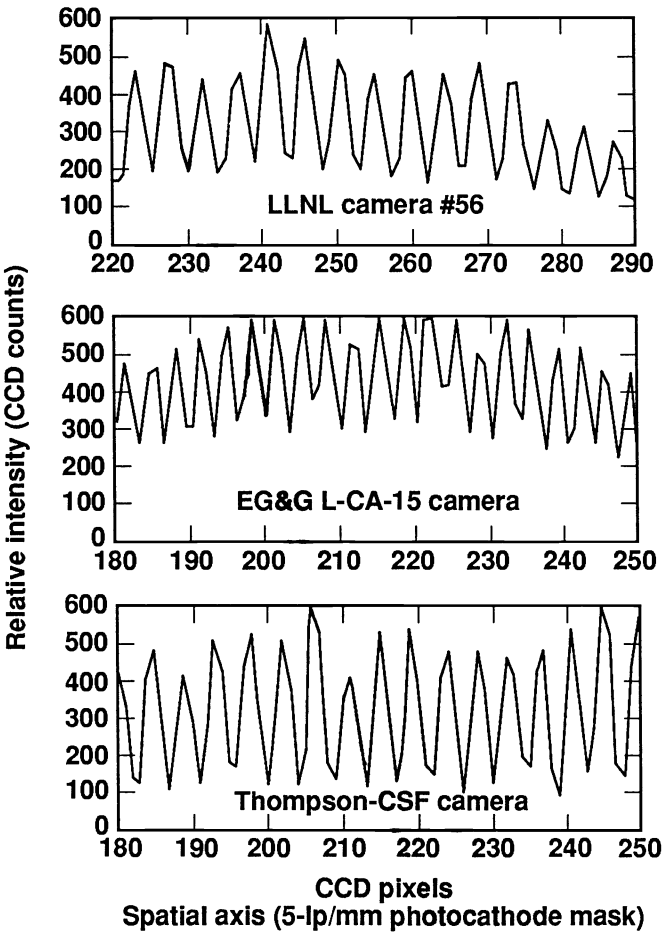

Figure 5. Comparative spatial resolutions.

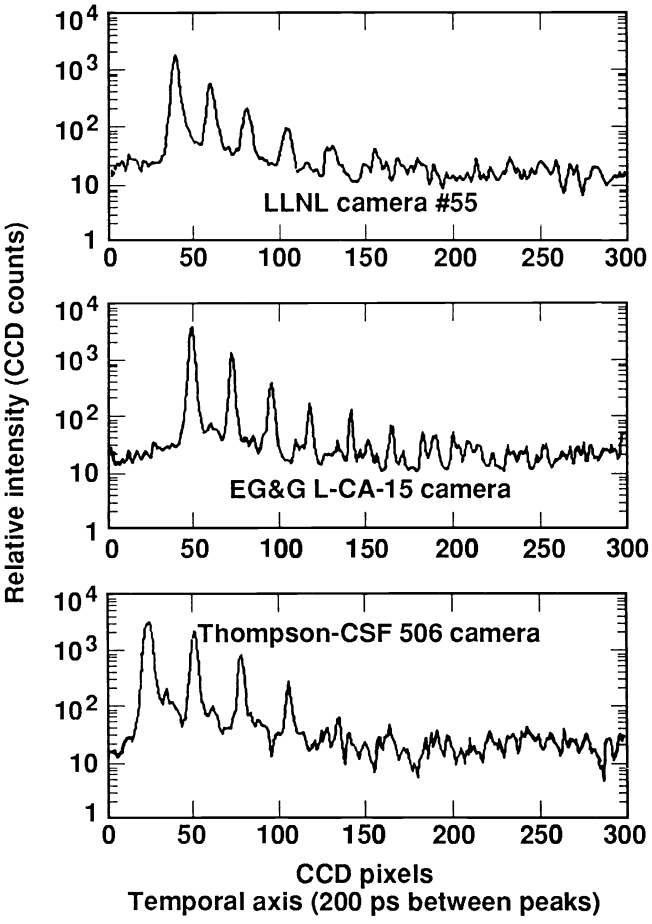

Figure 6. Comparative temporal resolutions.

We analyzed the temporal resolution by considering spatially narrow image portions (11 columns) covering at least 2 input channels and extending over the entire temporal extent, which was again limited by the size of the CCD array. These image portions were averaged by adding the columns together, effectively producing the average temporal history of the input channels. Such data at comparable intensity levels for all three cameras appear in Fig. 6. All three plots demonstrate at least a factor of 100 in signal range, and close examination reveals that the Thomson/ITT and EG&G cameras exhibit faster temporal response. The EG&G camera appears to carry its fast temporal response into the higher intensity pulses much more effectively. Further, the EG&G camera appears to demonstrate a higher peak-to-valley ratio.

The apparently high peak-to-valley ratio and signal range of the EG&G camera is more clearly demonstrated by the temporal profile of the somewhat brighter etalon-pulse train shown in Fig. 7. Here, the signal range displayed on a single streak record is in excess of a factor of 300. It can be seen that the most intense pulse is suffering some temporal response degradation.

In Figs. 6 and 7, the exponentially decaying etalon-pulse train should appear linear; this assumes that there is no etalon-pulse walk-off taking place. Some apparent nonlinearities in these data may be explained by such a walk-off created by misalignment of the etalon.

We have analyzed the temporal response of cameras with both the ITT and EG&G tubes by considering many etalon decay records. We compiled records for each camera to approximate relative dynamic range. All of the records for the Thomson/ITT camera were obtained at the same MCPI electronic gain of 145 (which was found to be nearly optimum in an earlier evaluation[3]). The streak records of the EG&G camera were obtained at electronic

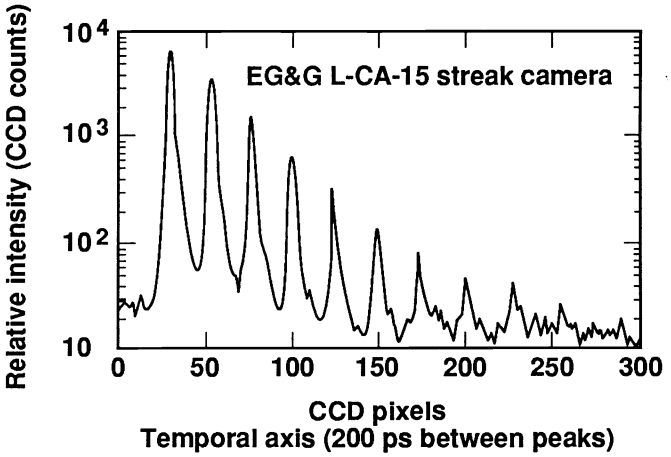

Figure 7. An example image from an EG&G camera, demonstrating an overall brighter image (high dynamic range).

gains ranging from 12 to 490, while those for the LLNL/ITT camera ranged from 7 to 125. Since we were interested in the temporal response of the streak tubes as a function of intensity, we normalized out the effects of the differing MCPI electronic gains by dividing the CCD counts at each impulse peak by the MCPI gain for each record. The resulting value, called P, then reflects the optical intensity at the phosphor screen for each pulse. Since we did not make careful radiant-gain measurements for each streak tube, we made no attempt to refer this intensity to the photocathode. As can be seen from Figs. 7 and 8, there is significant pulse spreading at the higher input intensities. Since we are interested in understanding the temporal response as a function of input intensity, we would ideally like to plot the pulse width vs the integral of each pulse. A reasonable approximation to this integral is the peak height, as recorded, times the pulse width. Therefore, Fig. 8 is presented as $P\Delta t$ vs Δt, where Δt equals the temporal pulse response (FWHM).

From Fig. 8, it is apparent that the time responses of the EG&G and Thomson/ITT cameras are comparable, as they both approach the ideal system limit of 2 CCD pixels (~15 ps FWHM), until a normalized intensity of slightly less than 1000 is reached. At approximately this intensity, the time response of the Thomson/ITT begins to exceed 20 ps, while the EG&G camera's temporal response apparently does not exceed the 20-ps mark until the input intensity reaches 3000 normalized counts. For both tubes, the temporal response is markedly degraded at the higher intensities. This intensity-dependent, temporal-response degradation is usually ascribed to space-charge effects within the streak tube.[6] The lowest discernable signals for each camera are included in Fig. 8.

If this pulse spreading is solely a result of space-charge effects, then the total amount of energy in each pulse should be conserved. To test this hypothesis, we prepared the data of Fig. 8 in a different form. Again, we used $P\Delta t$ to approximate the pulse integral and applied it to each pulse in the etalon pulse-train records. We then plotted these values as a function of time along the etalon pulse train, on a log-linear plot. The result appears in Fig. 9. Since the etalon decay is ideally exponential, these plots should be linear.

When we reduced the data, we had to account for variations in the instantaneous sweep rate that were caused by deflection nonlinearity. The LLNL/ITT camera probably needed fine tuning to improve the overall fidelity. Analysis of data from that camera demonstrates a 20% deflection nonlinearity, but it is not unreasonable to expect that its deflection linearity could approach that of the Thomson-CSF camera, which has less than 10% nonlinearity. The EG&G camera has demonstrated a nonlinearity less than 10% for the center 40 mm of the deflected image.

An earlier EG&G streak camera and streak tube (differing only in the type of phosphor used) was characterized without the use of an MCPI. Film was used to record the streak. Figure 10 is representative of the results of

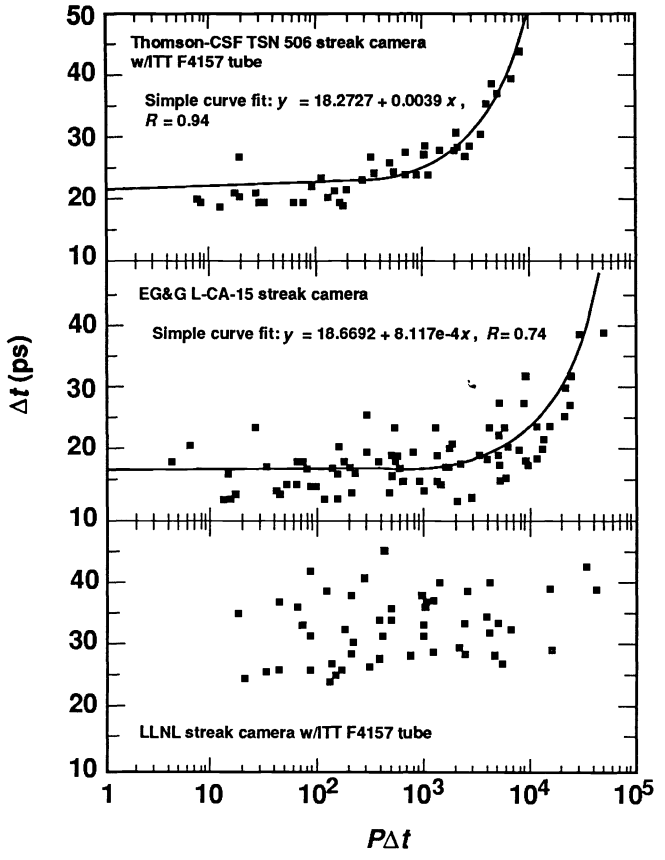

Figure 8. P values are equivalent to the CCD counts normalized by the MCPI gain settings (i.e., to the streak-tube phosphor intensity. Δt is the FWHM value of the individual pulses recorded.

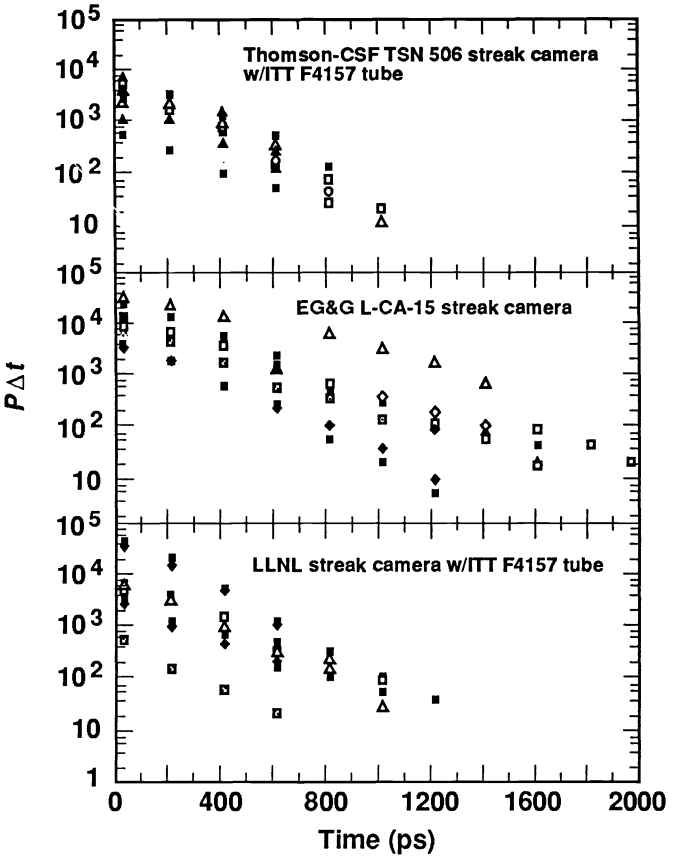

Figure 9. Normalized pulse energy vs time. $P\Delta t$ is an approximation of the pulse integral. (See Fig. 8 for a definition of $P\Delta t$.

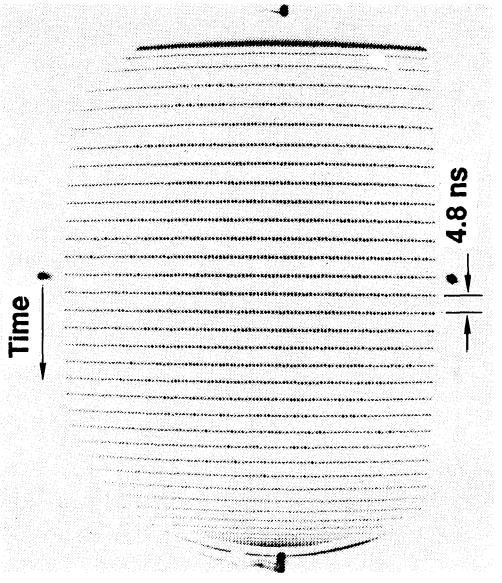

Figure 10. An example of an EG&G tube image without an MCPI, demonstrating space charge and shading across page (data from a previous, unreported evaluation).

this earlier work, which was not reported until now. The photocathode mask consisted of a row of rectangular apertures similar to those previously described, except with half the spatial frequency (2.5 lp/mm in the spatial direction). The input 610-nm light source was a mode-locked laser-pulse train with 15-ps FWHM pulses every 4.8 ns and an intensity high enough to cause noticeable temporal broadening. An etalon was not used for this image. We have determined the noticeable changes in the temporal response across the image to be a result of changes in the sweep speed along the temporal axis of the tube as the image is deflected. Figure 10 also shows that some change in the temporal width along the spatial axis occurs, but the source input to the photocathode along the spatial axis was not necessarily uniform along the length of the mask. This figure also illustrates some barrel (negative) image distortion and significant sweep nonlinearities at the extremes of the sweep. Since the MCPI limits the field of view, some of the off-axis information would typically be masked. An image gathered in the same manner as that in Fig. 10, except with attenuated laser pulse levels, was examined to determine if significant intensity shading is also present. By taking a slice of the image in the temporal direction (and averaging along the spatial direction, similar to the procedure used in Fig. 6), we found this shading to be very much in evidence (see Fig. 11).

7. DISCUSSION

Image-transfer characteristics of MCPIs affect spatial resolutions and, to varying degrees, the temporal resolution of a streak-camera system. Because of the different magnifications of the streak tubes and the different resolution values of the individual MCPIs, the results of spatial resolution in this evaluation are convoluted. That is, lower streak-tube magnifications imply higher output spatial frequencies, as demonstrated in Fig. 5. Some researchers have estimated that a point light source applied to the photocathode of an MCPI could influence the resulting output image as far as 1 mm away from the peak output intensity.[9] With a CCD readout camera that has high resolution and dynamic range, it easy to see that this could limit the depth of intensity modulation observed at the MCPI output when signals are close together.

The physical separation of the peak output signals along the temporal axis of the MCPIs, which result from individual laser impulses, were about 1.31 mm for the EG&G camera, 1.67 mm for the Thomson-CSF camera, and 1.34 mm for the LLNL/ITT camera. As long as the sweep rates are similar and the time between laser pulses is consistent, the effects of the MCPI on temporal resolution should be similar for each setup. High signal population comes at the price of adjacent channel interference.

Although every effort was made to attain an optimum relay lens focus, there was still a margin for error. Comprehensive flat-field studies have not been done on the CCD/relay lens combination, but the transmission shading is estimated to be near 25% across the 40-mm-diameter object plane (or image on the MCPI phosphor).

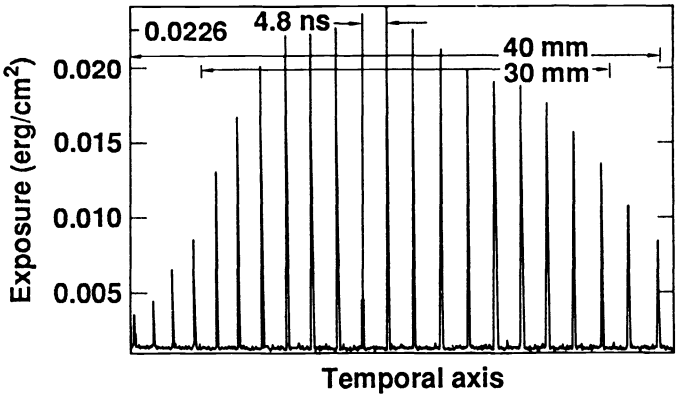

Figure 11. Sensitivity shading along the temporal axis from an EG&G L-CA-15 streak camera (data taken on 1/19/87).

It should be noted that both the temporal and spatial resolution are close to becoming limited by the input spot size of the mask on the photocathode. Some of the present data may be slightly affected by this limitation. In future measurements, a smaller aperture should be considered. Also, the opacity of the mask was approximately equivalent to a 4.3 ND filter. Since this mask was not completely opaque, some of the transmitted light may have acted to raise the noise floor for the recorded images.

In the course of data analysis, we determined that the laser footprint had significant hot-spots, which "walked around" the spatial direction with time. This beam walk-off may account for the scatter in Figs. 8 and 9. Because of unwanted feedback into the laser dye cavity, which results in mode-locking synchronization loss and other problems, the etalon could not be aligned perpendicular to the laser beam in this experiment. The small angle at which the etalon was canted and the distance (~4 ft) from the etalon to the streak camera photocathode determined how well the pulse train tracked the photocathode mask.

We recommend that future systems incorporate an isolation device such as a Faraday rotator between the laser and the footprint on the mask and that the etalon be positioned to prevent pulse walking. Hot-spot imperfections in the profile of the laser beam were spatially increased by expansion of the beam and by cylindrical lenses. Finally, a spatial filter is needed to more evenly distribute the laser energy along the length of the mask without temporally broadening the optical pulses.

It is possible that the laser system did not provide a depth of intensity modulation that greatly exceeded the dynamic range of these streak-camera recording devices. Some intensity structure between the main laser-light pulses seen by the streak camera at least partially resulted from uncoated optical components. To improve the source quality, we recommend that antireflective coatings be placed on all lens and filter surfaces or that they be tilted to avoid reflections whenever possible.

Unfortunately, the data taken in this evaluation was not all gathered in one day. Because the laser system is sensitive to almost any environmental change, stability was a problem. Although the average laser power appeared stable, we have data from consecutive acquisitions that demonstrate significant intensity variations. Independent diagnostics for these pulse-to-pulse variations are difficult to realize. The streak camera itself may be our best tool.

8. ADDITIONAL CONSIDERATIONS

The peak intensities attainable from the EG&G camera were much greater than from ITT-tube-based cameras tested under similar conditions. This effect may be the result of a combination of higher radiant gain, sharper temporal focus ($M = 0$), or better photoelectron emission associated with higher photocathode conductivity (see Fig. 7).

Frequently, a streak camera image may have geometric distortions[10] caused by a number of things, including misalignment of electrodes within the streak tube, improper voltages at the electrodes of the streak tube, or design characteristics of the individual streak tube. Some geometric distortions can be removed during data reduction, although this can be extremely time consuming. We did not attempt to remove geometric distortions, and we do not believe they affect our conclusions.

A disadvantage to a curved output optic is that geometric barrel (negative) distortion (evident in Fig. 10) and intensity shading may be introduced. We scanned images from the EG&G camera and the ITT streak tube along the center temporal axis of the output to determine if there was noticeable shading. The image from the EG&G camera with the P-11 phosphor screen (shown in Fig. 11) exhibits a shading of about 45% over a 30-mm length. Shading of an image from an ITT streak tube operated in the streaked-image mode was less than 5% across 30 mm of deflection. (Data for this test are not presented here.)

Both tubes have remotely processed photocathodes, which provide more uniform spectral response across the active photocathode area and less internal contamination from cathode materials than do tubes that have cathodes processed in situ. Both of the cameras that use the ITT tube are designed to allow periodic checks to look for

cathode-sensitivity changes. Because the cathode and accelerator electrodes in the EG&G tube are capacitively coupled, it is not possible to conveniently measure photocathode sensitivities.

Some experiments at LLNL require up to 3 mm of active photocathode area across the time axis of the input window. These experiments temporally multiplex a number of fiber channels to conserve space.[11,12]

9. CONCLUSIONS

In our preliminary comparison of the ITT model F4157 streak-tube-based cameras and the new EG&G model L-CA-15 streak camera, we analyzed the operation of each camera and the appraised the test setup. Characteristics evaluated for each camera included time response, spatial resolution, and dynamic range. Typically, each system described in this report is capable of recording more than 80 photonic data channels with high temporal and spatial fidelity (5-lp/mm). All of the cameras are capable of 5-GHz operation over a dynamic range of 100:1. The number of usable channels is limited by the permissible adjacent channel cross talk.

The overall fidelity of the LLNL/ITT camera was inferior to the Thomson/ITT camera, partly because little time was allotted for fine tuning the electronics in the LLNL/ITT camera.[13] However, there may be significant performance differences between the two ITT streak tubes; this issue will remain unresolved until more tubes can be characterized.

The two types of streak tubes exhibited similar time responses under our test conditions. However, the EG&G tube demonstrated a greater high-speed signal range and an impulse response with a cleaner signal extinction than the ITT tube-based cameras, but at the expense of poorer spatial resolution, significant intensity shading, and additional geometric distortion. We believe that further characterization of several tubes of each type, as well as upgrades to our characterization system, should be carried out to ensure the validity of these conclusions.

This evaluation did not exercise the large number of system variables; therefore, many unanswered questions remain. However, we have discovered ways to improve measurement technique applicable to future work.

10. ACKNOWLEDGMENTS

We thank Fred Schumacher for his skillful operation of the laser system and Greg Lancaster for his adept assistance in the setup of the input lens and CCD readout system. We also thank Alan Teruya for the use of some of his IDL macros.

This work was performed under the auspices of the U.S. Department of Energy by the Lawrence Livermore National Laboratory under contract number W-7405-ENG-48.

11. REFERENCES

1. R. A. Lerche, E. L. Grasz, and R. L. Griffith, *5-GHz Operation of the ITT and RCA Streak Tubes with a 7.5-NS Time Window*, Lawrence Livermore National Laboratory, Livermore, CA, UCID-21264 (1987).
2. C. K. Hinrichs and R. W. Olsen, *A High-Spatial-Resolution Streak Image Tube*, EG&G Inc., Pleasanton, CA, EGG-10282-4049 (1985).
3. M. Lowry et al., "Characterization of a Large-Format, High-Fidelity, Picosecond, Optical Streak Camera," *Proc. SPIE* **832** (1987).
4. C. C. Lai et al., "Design and Development of a New Streak Tube," Lawrence Livermore National Laboratory, Livermore, CA, *E.E. Technical Review*, UCRL-50025-86-1 (1986), pp. 1–12.
5. T. Jennings et al., *Test Results, EG&G San Ramon Streak Tube and Test Results, ITT Streak Tube*, EG&G Energy Measurements, Los Alamos, NM (1987).
6. R. Kalibjian, "Space-Charge Temporal Broadening Effects in Streak Camera Tubes," in *Proc. 13th Internat. Cong. High-Speed Photography, Tokyo, JA*, (1978), pp. 452–455.
7. J. D. Wiedwald and R. A. Lerche, "Streak Camera Dynamic Range Optimization," *Proc. SPIE* **832** (1987).

8. R. J. Korniski, *2.5:1 Relay Design NAO = 0.245, Final Report*, prepared for LLNL by Optical Research Associates, Pasadena, CA (1985).
9. J. D. Wiedwald, "Veiling Glare in the ITT F4113 Image Intensifier," *Proc. SPIE* **981** (1988).
10. D. S. Montgomery, R. P. Drake, B. A. Jones, and J. D. Wiedwald, "Flat-Field Response and Geometric Distortion Measurements of Optical Streak Cameras," *Proc. SPIE* **832** (1987).
11. R. P. Reedy, F. Roeske, and D. E. Smith, "Fiber-Optic Spectral-Streak Equalizer," *Rev. Sci. Instrum.* **56**(7), 1356 (1985).
12. F. Roeske, D. E. Smith, B. L. Pruett, and R. P. Reedy, "A High-Bandwidth, Multichannel Fiber-Optic System for Measuring Gamma Rays," *Proc. SPIE* **506**, 29 (1984).
13. R. A. Lerche et al., "Resolution Limitations and Optimization of the ITT F4157 Streak Tube Focus for Fast (10-ps) Operation," *Proc. SPIE* **981** (1988).